ISSN 1005-9784
CODEN JCSTFT

JOURNAL OF CENTRAL SOUTH UNIVERSITY OF TECHNOLOGY

Available online
www.springerlink.com

Central South University Press
www.csupress.com.cn

Springer

J. Cent. South Univ. (2016) 23: 1633−1642
DOI: 10.1007/s11771-016-3218-6

Springer

Performance analysis of a pneumatic to servo converted system for electrode actuation in resistance spot welding using 304L austenitic stainless steel

Nachimani Charde

Department of Mechanical Engineering, Faculty of Engineering, University of Malaya, 50603 Kuala Lumpur, Malaysia

Abstract: A high current, AC waveform controller with C-type body frame of spot welder (75 kVA), was examined for the electrode actuating system whose pneumatically driven system has been redesigned and refitted for the servo based system without any vertical spring assistance in the 50 mm movable distance. Moreover, the pressing mechanism was carefully handled during the entire pressing tasks as to ensure that no catastrophic reaction happens for the electrodes' caps, electrodes' holders as well as the other part of mechanical assembly. With the mechanically originated-pneumatic and also the converted-servo systems, the stainless steels are welded for both systems to characterize the improvements. While the welding processes were carried out, the electrical signals have been captured to compute the signals' representation of entire sequences. Later, the welded samples were underwent the tensile shear test, metallurgical observation and hardness test. The analytical results show distinct changes in the force profiles which has led to profound changes in mechanical properties of welded specimens.

Key words: force profiles; electrode actuation system; servo and pneumatic system

1 Introduction

An excellent weld formation basically relies on the proper setup of process-tuning parameters in any resistance spot welding technique. The weld formation is established due to its process-tuning parameters; specifically the electrical current, current flowing time, electrode pressing force and the electrode cap's contact areas [1−3]. To understand how the tuning of parameters works within the welding lobe diagram, two out of four parameters are kept unvaried while changing the other two parameters concurrently to determine the proper window (see Figs. 2(a) and (b)). There are numerous discussions available to support either pneumatic alone or servo alone separately but there is inadequate information available about the electrode actuating system that converted from either pneumatic to servo or vice versa. These two systems have dissimilar characteristics in terms of force stimulations as far as the pressing mechanism is determined [4−6]. Force distributions are usually measured from the squeezing moment, passing through the welding moment and finally ended up after the solidification process ends. In this experiment 1-mm stainless steels were welded using pneumatic based and re-designed servo based (National Instrument's Lexium 23 category) electrode actuation system respectively. During the entire welding process, the inherent process behaviors such as the electrode terminal voltage, the welding current and electrode pressing force are recorded with signals detectors [7−8]. Based on these measured signals, the static and dynamic resistance, heat generation distribution and force profiles are computed for both systems. Finally, the welded samples underwent the tensile shear test to compare the weld diameters' increment and observed for metallurgical alteration and measured for the hardness changes [9−11].

2 Experimental

Welding samples were made of 304L stainless steel, with a rectangular size of 200 mm length by 25 mm width, utilizing the 1-mm thickness materials. The original chemical elements that found on stainless steel sheets were: w(C)=0.048%, w(Cr)=18.12%, w(Ni)=8.11%, w(Mn)=1.166%, w(Si)=0.501%, w(S)=0.006%, w(N)=0.053% and w(P)=0.030%. The original hardness of the stainless steel was HRB81.7 and tensile ultimate strength was 515 MPa. The test specimens were welded at one side of the end, with an alignment of 30 mm lap joint from one end, as shown in Fig. 1. The electrode tip applied to weld was with 5 mm diameter, manufactured as flat-round-face but truncated type, basically selected

Received date: 2015−06−12; **Accepted date:** 2015−09−22
Corresponding author: Nachimani Charde, Researcher; Tel: +60379674497; Fax: +60379675317; E-mail: nachicharde@yahoo.com

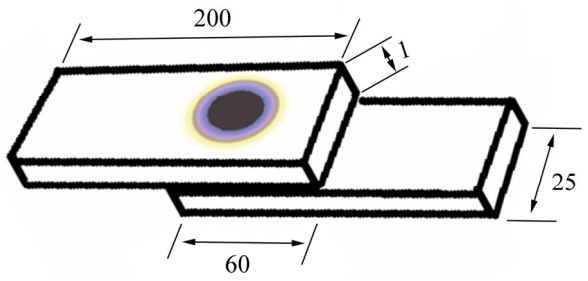

Fig. 1 Test sample (Unit: mm)

from the class two classifications of RWMA's class two-welding electrode category. The welding procedures are as common as how the other welding process takes place.

Welding-lobe diagrams determine the proper working region of process-tuning parameters for any thickness of weldable materials in RSW. The electric current, welding time, electrode force and electrode tip's size are the tuning elements that establish the relationship among them. Usually, two parameters out of total four parameters are varied in an attempt as to establish proper welds' regions or simply working window. Electrode force and welding current are gradually increased to form a relationship in this experiments and based on such activity, Figs. 2(a) and (b) were drawn. From Figs. 2(a) and (b), that the proper weld regions are marked with green boxes and enclosed with continuous line. Detailed explanations about the colors' representation and boxes are given in Figs. 2(a) and (b). With the use of these welding lobes' limits that marked with "X", a weld schedule was correspondingly tabulated (Table 1) therefore.

The entire welding process was accomplished in accordance with the combinations of process-tuning parameters, which is summarized in Table 1. Seven welded pairs were developed for each weld schedule as the first five pairs were used to the tensile test, sixth one was used for hardness test and the final one was used for metallurgical observation. As for the hardness test and tensile test, the Rockwell hardness tester using scale B and 100 kN tensile test machines were engaged to

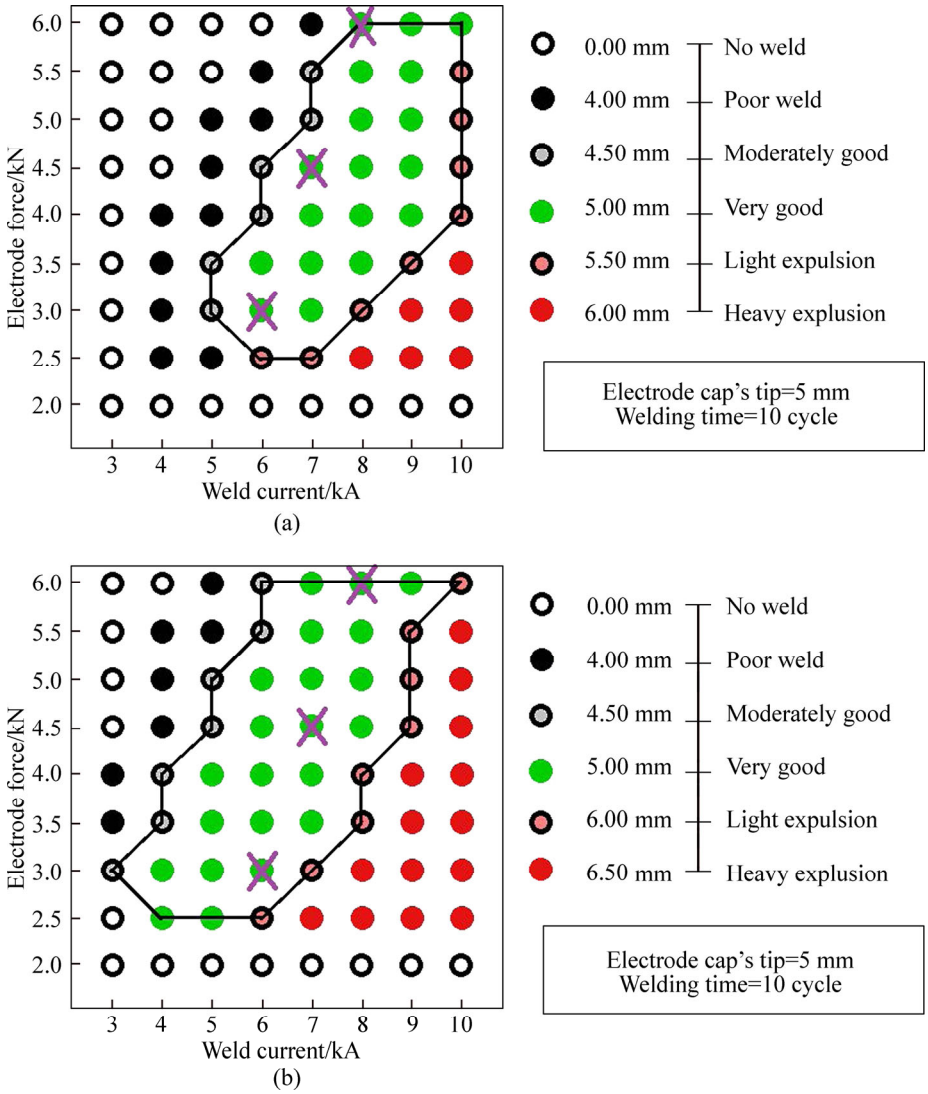

Fig. 2 Welding-lobe diagram of welding current against electrode force: (a) Pneumatic based system; (b) Servo based system

Table 1 Process-tuning parameters

Sample No.	Varied parameter		Unvaried parameter	
	Electrode force/kN	Welding current/kA	Welding times	Electrode cap's tip diameter/mm
1−7	3	6	10	5
8−14	3	7	10	5
15−21	3	8	10	5
22−28	4.5	6	10	5
29−35	4.5	7	10	5
36−42	4.5	8	10	5
43−49	6	6	10	5
50−56	6	7	10	5
57−63	6	8	10	5

complete the experiments. The V2A etchant which contains 100 mL water, 100 mL hydrochloric acid and 10 mL nitric acid was applied to etch the well prepared and weld polished bakelite-samples.

3 Results and discussion

3.1 Welding lobe diagrams and working windows

It is found that the servo based system has improved the working regions of welding lobe for 1 mm thickness of stainless steel as the working window has been widened up for good welds and pulled towards initial startup. Look at the green colored boxes in the welding lobe diagrams of both systems (Figs. 2(a) and (b)), with respect to its columns and rows, in pneumatic based system, the welding current against electrode force sets has produced 18 good welds whereas in the servo based system, the welding current against electrode force sets have produced 22 good welds. This is noticeable change for good welds in servo based system as it increases by 37% of the pneumatic based system's performance. Moreover, the light expulsion region starts at 5.50 mm for pneumatic based system but not same for the servo based system. In servo based system, the light expulsion starts at 6.00 mm of diameter. It should be noted here that the critical weld growth of stainless steel starts at $4\sqrt{t}$; where t stands for the thickness of base metal [12−13]. Although the critical weld growth of stainless steel starts at 4.00 mm for 1 mm thickness of two sheets, the servo based system has successfully maintained the light expulsion until the weld growth reaches about 6.00 mm of weld diameter. This factor has also to be seen in another aspect because the electrode tip's original diameter was 5 mm without any mushrooms or any other electrode deformation during welding process. If the electrode tip is with 5 mm of diameter and then the possibility of weld indentation has to be high if the molten area can reach up to 6 mm. This factor has been predominantly handled in the servo based system due to force profiles' consistencies.

3.2 Static resistance of both systems

Accessing the static resistance, it leads to the prediction of mismatch or misalignment of electrode caps as the path has sandwiched contacts of resistive components. Hence, the static resistance (R_1+R_2+R_3+ R_4+ R_5) has to be measured for both electrode actuating systems as to understand the contact resistances' changes because the force and the resistances are inversely related to each other within the good working region of welding lobe diagram (Fig. 3(a)). The contact resistances are measured from upper electrode cap towards all the way to the lower electrode cap with base metal placed-in-between [14]. It consists of five layers, where R_1 represents the contact resistance between upper electrode

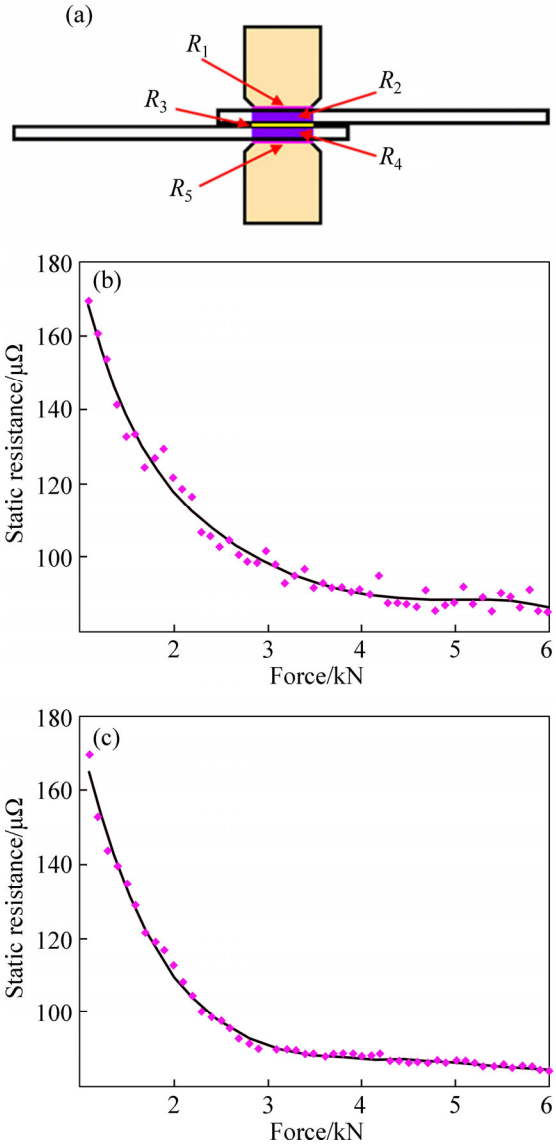

Fig. 3 Various resistive components in static resistance (a) and static resistance of pneumatic based system (b) and static resistance of servo based system (c)